

PAPER

Vacancy-assisted core transformation and mobility modulation of a-type edge dislocations in wurtzite GaN

To cite this article: Cheng Chen *et al* 2019 *J. Phys. D: Appl. Phys.* **52** 495301

View the [article online](#) for updates and enhancements.

You may also like

- [Pressure influence on bound polarons in a strained wurtzite GaN/Al_xGa_{1-x}N heterojunction under an electric field](#)
Zhang Min and Ban Shiliang
- [First-principles investigation of a-line Shockley partial dislocations in wurtzite GaN: core reconstruction and electronic structure](#)
I Belabbas, G P Dimitrakopoulos, J Kioseoglou *et al.*
- [Electron spin relaxation in two polymorphic structures of GaN](#)
Nam Lyong Kang



The Electrochemical Society

Advancing solid state & electrochemical science & technology

DISCOVER
how sustainability
intersects with
electrochemistry & solid
state science research



Vacancy-assisted core transformation and mobility modulation of a-type edge dislocations in wurtzite GaN

Cheng Chen^{1,2}, Fanchao Meng², Huicong Chen², Pengfei Ou²,
Guoqiang Lan², Bing Li³, Qiwen Qiu² and Jun Song^{2,4}

¹ School of Aeronautics, Northwestern Polytechnical University, Xi'an 710072, Shaanxi, People's Republic of China

² Department of Materials Engineering, McGill University, Montréal, Québec H3A0C5, Canada

³ School of Engineering, Huzhou University, Huzhou 313000, People's Republic of China

E-mail: jun.song2@mcgill.ca

Received 13 May 2019, revised 11 August 2019

Accepted for publication 29 August 2019


Published 18 September 2019



Abstract

In this study, core structure dependent dislocation dynamics of a-type edge dislocation in three slip systems (basal, prismatic and pyramidal) of wurtzite GaN have been investigated using classical molecular dynamics simulations. All potential a-type edge dislocation cores in the shuffle and glide planes of the three slip systems have been identified, and the corresponding dislocation dynamics were examined. Our calculations reveal that for all of the three slip systems, all of the shuffle cores are planar glissile and mobile, while being non-planar sessile and immobile for all of the glide cores. We further show that vacancy can be used to activate the motion of glide cores via core transition from glide to shuffle, which is also valid for AlN and InN. The critical shear stresses for the motion of glide cores are also determined at various vacancy concentrations. Our study clarifies core structure dependent dislocation dynamics characteristics and provides ways in tuning dislocation motions in wurtzite crystals.

Keywords: GaN, dislocation dynamics, dislocation cores

 Supplementary material for this article is available [online](#)

(Some figures may appear in colour only in the online journal)

1. Introduction

The nucleation and propagation of high density of threading dislocations are essential entities in the optoelectronic and protective coating applications of gallium nitride (GaN) and its compounds [1–14]. It is well known that the dislocations in GaN can propagate along the epitaxial direction and annihilate in pairs and their density varies with increasing epitaxial layer thickness [15–17]. They are regarded as critical factors that degrade the lifetime and overall efficiency of GaN-based light-emitting and high-power electronic devices, due to the potential dislocation-related non-radioactive recombination [18] and current leakage paths [19–22]. In addition, plastic

deformation in GaN in response to external stress mainly occurs via dislocation motions [23], and their gliding and climbing characteristics are closely related to the wear performance of GaN-based coating layers [9, 24, 25]. Consequently, in order to ensure reliable and enhanced material properties and performance, there is critical need to control the nucleation and propagation of dislocation in GaN, which in turn necessitates detailed knowledge of the structures, characteristics and dynamic behaviors of dislocations.

Numerous potential stable dislocation core structures in wurtzite GaN, identified from experimentation [26–28] and/or atomistic simulations [29–36], have been reported. In general, they can be classified into three main groups: dislocations with (i) a-type, (ii) (a+c)-type and (iii) c-type Burgers vectors. For each group, the dislocation cores can be further categorized

⁴ Author to whom any correspondence should be addressed.

into the glide and shuffle sets, which correspond to two parallel yet inequivalent families of slip planes, with the former centered in-between narrowly spaced atomic layers, while the latter centered in-between widely spaced atomic layers [36, 37]. Yet in contrast to the great efforts in understanding and characterizing the dislocation core structures in wurtzite GaN, there has been very limited investigation of dislocation dynamic behaviors, and their dependence on the core structure [23, 29, 38–41]. For instance, even for the simplest case of a-type edge dislocations, only the mobilities of shuffle cores have been studied, but no analyses were conducted on the glide cores [29, 42], not to mention other more complicated dislocation cores.

The present study aims to contribute to addressing the afore-mentioned knowledge deficit. Employing molecular dynamics (MD) simulations, potential a-type edge dislocation cores in the shuffle and glide sets of the three slip systems (basal, prismatic and pyramidal) of wurtzite GaN have been constructed and systematically examined. Our results reveal that in the three slip systems, the dislocation motions are strongly core structure dependent, with the shuffle cores being mobile, while the glide cores being largely immobile due to their extended core structures. It was demonstrated that motions of the immobile glide cores can be enabled via a climb-glide process, which can be facilitated by a vacancy-assisted core transition mechanism. The effect of vacancies on glide cores was further analyzed by examining the threshold stress required for inducing dislocation motions. We further showed that such phenomena are also generally valid for other wurtzite structures, i.e. AlN and InN. The present study provides valuable inputs for understanding and engineering of dislocation behaviors in wurtzite structured materials.

2. Computational methodology

The simulations of dislocation core structures and dynamics in GaN were performed in the framework of classical molecular dynamics (MD) implemented in the LAMMPS package [43]. The interatomic interactions are described employing the Stillinger-Weber potential [43–48] for GaN [49]. This interatomic potential been demonstrated to accurately predict a wide variety of physical properties of GaN, including the crystal structure, lattice parameters, elastic constants, and defect characteristics [50] under stoichiometric conditions, and has been previously applied in mechanical assembly [6], strain relaxation of misfit dislocations [6, 46], substitutional diffusion [50] and heteroepitaxial growth [51].

Typical shuffle and glide cores of a-type edge dislocations (of Burgers vector $\vec{b}_1 = 1/3[1\ 1\ \bar{2}0]$) identified in the three slip systems, basal ((0001)[11 $\bar{2}$ 0]), prismatic ((1 $\bar{1}$ 00)[11 $\bar{2}$ 0]) and pyramidal ((1 $\bar{1}$ 01)[11 $\bar{2}$ 0]), of GaN, were considered. A rectangular supercell containing an edge dislocation is used, with its three mutually perpendicular axes denoted as \vec{x}_1 , \vec{x}_2 and \vec{x}_3 respectively. The dislocation was generated at the center of the supercell through displacing atoms in the supercell according to the elasticity theory [52, 53]. The supercell has free boundary condition along \vec{x}_3 , while periodic along \vec{x}_1

and \vec{x}_2 (see figure 1), which coincide with the dislocation line and Burgers vector directions, respectively. The supercells are of dimensions 15.7 nm \times 15.2 nm \times 5.1 nm along \vec{x}_1 , \vec{x}_2 and \vec{x}_3 directions respectively for the basal and prismatic slip systems, but 15.7 nm \times 15.2 nm \times 7.1 nm for the pyramidal slip system. The atomic configurations of core structures obtained for a-type edge dislocations in the three slip systems are illustrated in figures 1(a)–(c). In the search of all possible dislocation core structures, the core origin was initially placed at different locations, and the dislocation core subsequently constructed was relaxed via energy minimization using the conjugate gradient (CG) algorithm⁵ [54], with the locations leading to different core structures identified. As shown in figure 1, four types of dislocation cores have been identified, labelled by I, II, III and IV. Specifically, type I cores correspond to dislocation cores located at shuffle planes while types II, III and IV cores correspond to dislocation cores located at glide planes. Thus hereafter we refer to type I cores as shuffle cores while types II, III and IV cores as glide cores for simplicity.

Following the energy minimization, the system was then further relaxed within the isothermal-isobaric (NPT) ensemble to raise the temperature to 300 K over duration of 2 ns. Then the system was maintained at 300 K for 3 ns till zero stress conditions were ensured along all periodic directions. Subsequently, the shear stress has been applied to the top and bottom atom slabs, being the two outmost slabs of thickness ~ 0.7 nm along the non-periodic direction \vec{x}_3 , with equal but opposite magnitudes to drive the dislocation to move. The timestep of one femtosecond (fs) has been set for all simulations.

3. Results and discussion

From the responses of different dislocation cores in the three slip systems under the application of shear stress, we found that the shuffle cores are planar mobile glissile cores, and would start to move once the applied stress is beyond the critical stress, the values of which are 0.1 GPa, 0.1 GPa and 6 GPa for basal, prismatic and pyramidal slip systems respectively. On the other hand, most glide cores are non-planar immobile sessile cores regardless of the shear stress applied (i.e. the glide core remains immobile even when the applied stress goes beyond the failure stress). However, there exists one exception in the glide set, i.e. the pyramidal type-IV core, which can undergo transformation into a shuffle (pyramidal I) core to become mobile upon the application of large shear stress ($> \sim 6$ GPa).

This drastic difference between these two core groups may be attributed to the fact that all glide cores have an extended core structure (see figure 1) that spans beyond the glide plane into the neighboring plane(s). Consequently motions of a glide core would require slip displacement for atoms in more than one plane, rendering it not possible (or difficult) to occur.

⁵ Note: the conjugate gradient algorithm was complemented by other minimization algorithms/convergence criteria to ensure the elimination of artificial core structures.

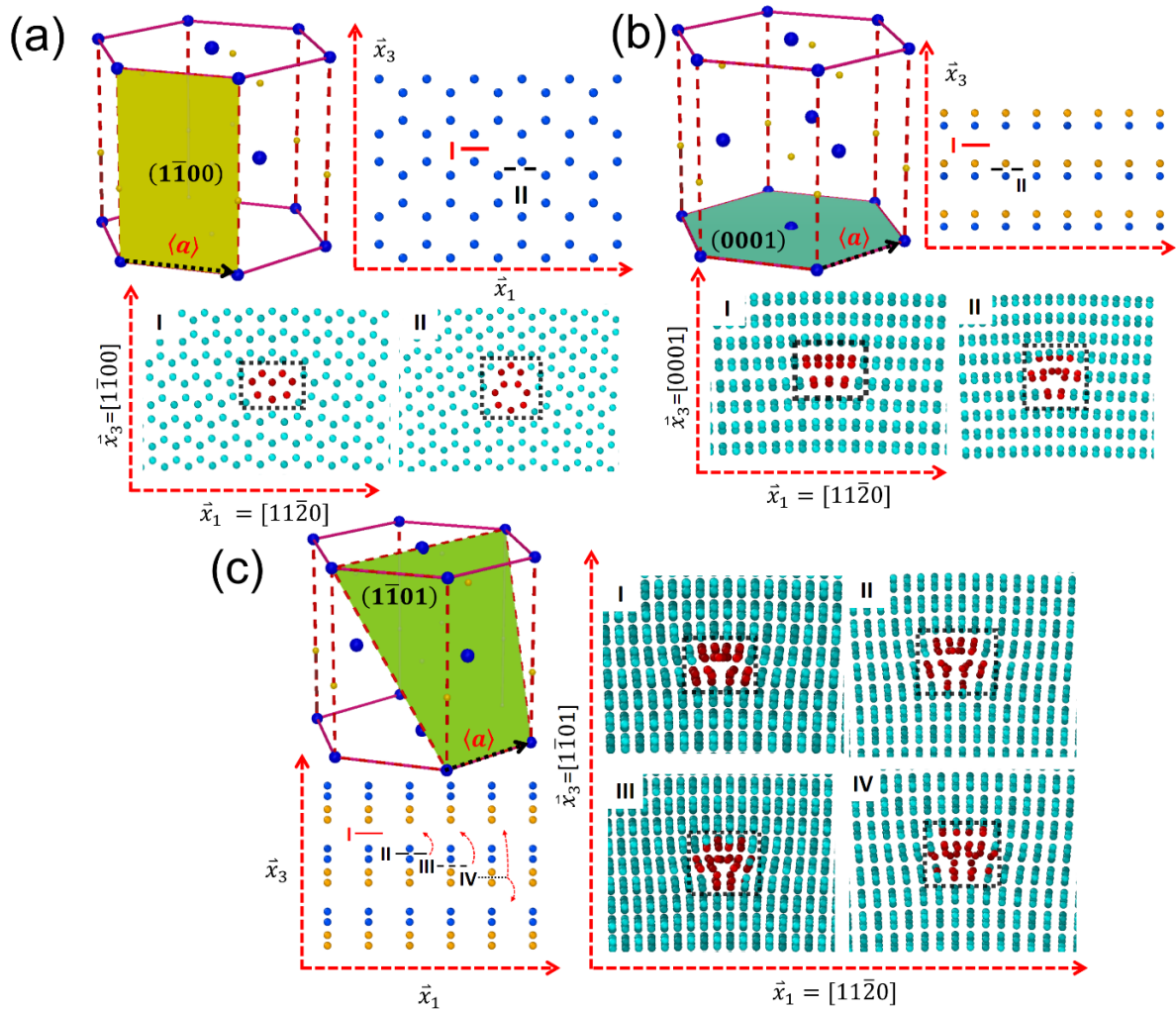


Figure 1. 3D schematic illustrations of the three slip systems, (a) prismatic, (b) basal and (c) pyramidal, where the shaded plane indicated the slip plane. The Ga and N atoms are indicated by blue and golden spheres respectively. The shuffle (indicated by the red solid line of label I) and glide slips (indicated by black dashed, short dash and dash-dot lines of labels II, III, and IV respectively), and the corresponding projection views of dislocation cores structures are also illustrated, with core atoms colored red. The curved red dash arrows in (c) show the different distances the three types of glide cores need to climb up or down to the neighboring shuffle planes.

Such core-dependent dislocation dynamics behaviors are well illustrated in figure 2 showing the response of a representative edge dislocation (in the prismatic slip system) consisting of mixed glide and shuffle line segments. As seen from figure 2, upon the application of shear stress, the shuffle segment moves while the glide segment stays immobile to pin the dislocation. Consequently, this results in dislocation bow-out and eventually dislocation loop formation upon further stress application. Similar behaviors can also be observed for edge dislocations with mixed core structures in other basal and pyramidal slip systems. The dislocation pinning/bowing-out picture shown in figure 2(a) also suggests that *a*-type edge dislocations of mixed shuffle/glide components can serve as sources for continuous dislocation loop generation, thus contributing to the existence and propagation of high-density dislocation loops in growing GaN crystal [26–28, 55].

The above results indicate an interesting possibility of modulating dislocation activities by controlling the core structure. Examining the shuffle and glide cores, we can easily see that they may undergo transformation into each other via the dislocation climbing process, which is a non-conservative process

that may be assisted by vacancies or equivalently self-interstitials [52]. As illustrated in the example case in figure 2, despite direct slip motions not accessible for glide cores, they may undergo a climbing process to transform into mobile shuffle cores, which would subsequently enable dislocation motions. In this regard, we further investigated the core transformation and its effects on dislocation motions. Given the equivalency of the roles of vacancies and self-interstitials in dislocation climbing, here we focus on vacancies for simplicity.

We consider glide cores where the core atoms, located in the region that is expected to be affected by the climbing process, were randomly replaced by vacancies, and examine their responses under shear stress. We found that, with the introduction of vacancies to the glide core, the shear stress indeed can drive a glide-to-shuffle core transition, subsequently allowing the whole dislocation line to move, as illustrated in figure 3. It is also worth noting in figure 3 that the dislocation motion after the core transition leaves behind some defects. These defects can be dislocation segments, small dislocation loops, individual or clusters of self-interstitials. The formation of those defects is well expected given

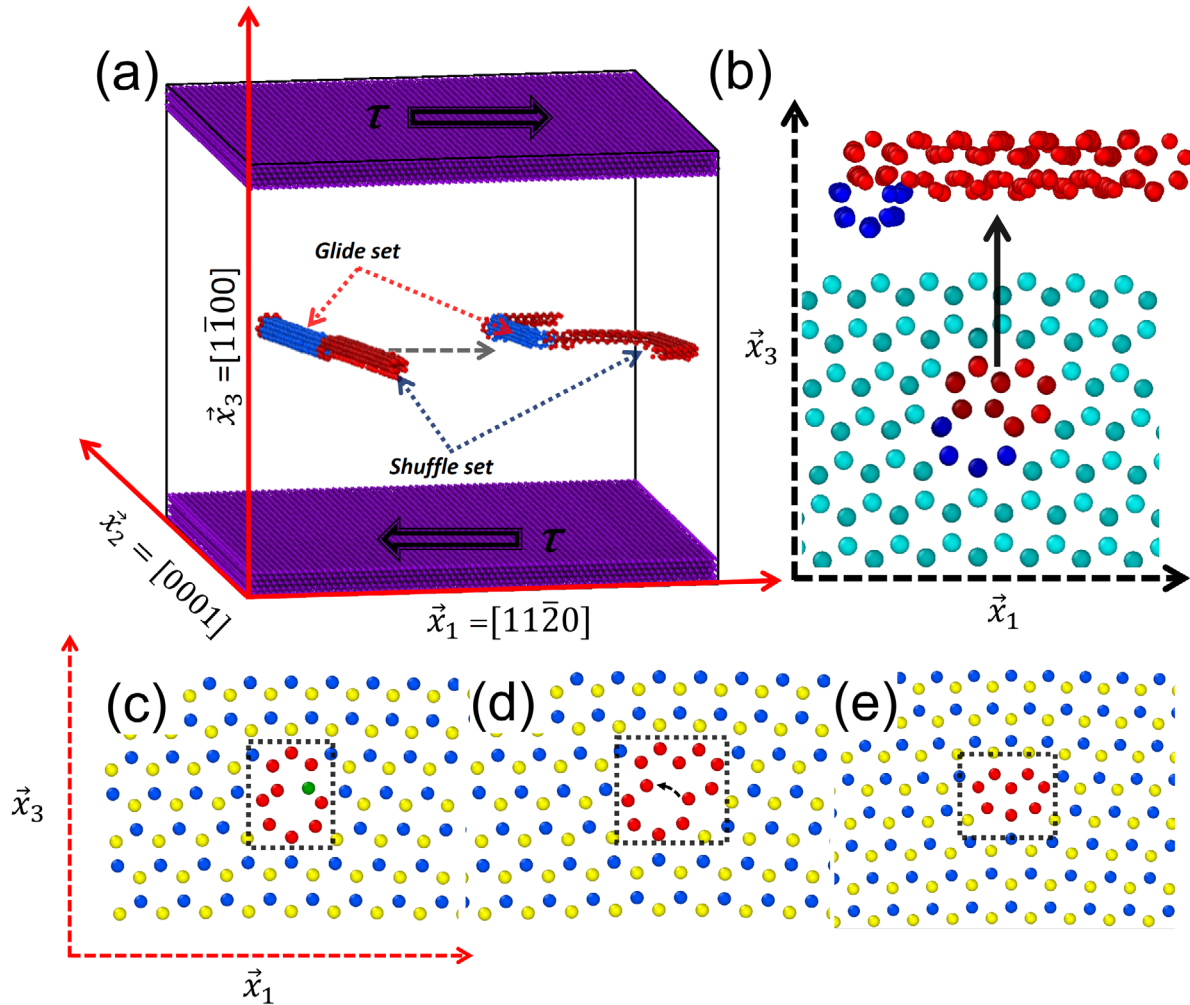


Figure 2. (a) 3D illustration of the simulation supercell containing an edge dislocation in the prismatic slip system which comprises of both glide (blue) and shuffle (red) line segments. Note that lattice atoms other than those in the dislocation core or fixed slabs are not shown for clarity. (b) A close-up projection view of the dislocation line in the initial straight, stress-free state (bottom) and curved state (top) upon the application of a shear stress. (c), (d) An example glide-to-shuffle core transformation, realized via dislocation climbing with the assistance of vacancies. (c), (e) The glide and resultant shuffle cores, while the arrow in (d) indicate the key atom displacement in the core during the transformation. In this example, vacancies were introduced to substitute the atomic sites colored green in (c). An atomistic animation showing the whole transformation process can be found in the online supplementary materials (stacks.iop.org/JPhysD/52/495301/mmedia).

that the vacancies introduced alone are not sufficient (in the sense of mass conservation) for a complete glide-to-shuffle transition throughout the whole dislocation line. Figure 4 shows the threshold stress σ_{th} required to completely move an edge dislocation initially of a glide core, as a function of the vacancy concentration c_v , defined as the percentage of core atoms substituted by vacancies. For glide cores in the basal and prismatic slip systems, we see the threshold stress exhibit a monotonic trend as the vacancy concentration increases, decreasing from $\sigma_{th} > 8$ GPa (for $c_v < 5\%$) to $\sigma_{th} < 400$ MPa (for $c_v > 95\%$). Meanwhile, for the pyramidal slip system where three different glide cores exist, we see that for glide cores of type II and III, the threshold stress also decreases as the vacancy concentration increases, like seen for the basal and prismatic slip systems, yet with the reduction to a much less degree and the threshold stress plateauing at 6 GPa for vacancy concentration beyond 50%. It is worth noting that this plateau stress of 6 GPa is precisely the stress required to

drive a pyramidal shuffle core to move. On the other hand, for the pyramidal glide core type IV, we see that the threshold stresses show a non-monotonic dependence on the vacancy concentration, being ~ 6 GPa for low (i.e. $c_v < 20\%$) and large ($c_v > 70\%$) vacancy concentrations, while fluctuating between 6 and 8 GPa for intermediate vacancy concentrations. Particularly intriguing is that the threshold stress peaks at vacancy concentration of $\sim 50\%$.

The contrast in the dependence of σ_{th} on c_v for different slip systems, as observed in figure 4, indicates different degree of difficulty in realizing the glide-to-shuffle core transition, and different structural evolution along the dislocation line direction, as will be elaborated in the following. For the basal and prismatic slip systems, the dislocation core possesses relatively simple structure and requires less degree of reconstruction during the glide-to-shuffle transition. Consequently the influence from the presence of vacancies is more straightforward and profound, as seen in figure 4. For the pyramidal

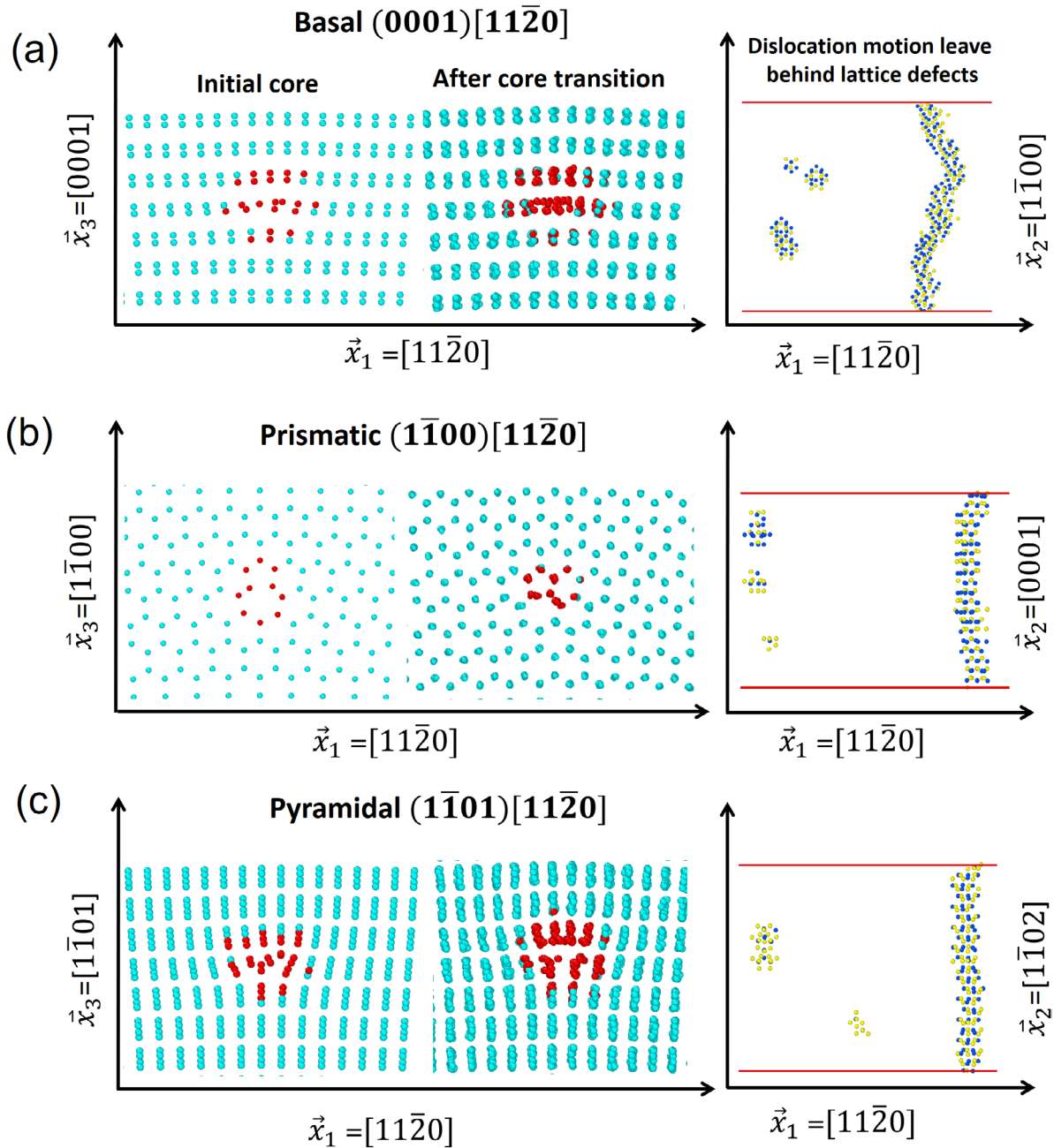


Figure 3. The representative vacancy-assisted glide-to-shuffle core transition, along with the subsequent dislocation motion for (a) basal, (b) prismatic and (c) pyramidal type III glide cores. With the vacancy concentration being 50%, the dislocation cores structures of initial state and after transition are colored in red while the other lattice Ga and N atoms are not shown for clarity. The top view in the rightmost parts show the left lattice defects after the dislocation slip with Ga and N atoms colored in yellow and blue spheres, respectively.

slip system, the dislocation core is more spread-out, spanning across more atoms planes compared to the ones in basal and prismatic systems. Moreover, as illustrated in figure 1, the introduction of vacancies would promote the glide core to climb upwards (along \vec{x}_3) to transform into a shuffle core. For pyramidal type II and type III glide cores, our simulations revealed that the core did exhibit an upward motion during the glide-to-shuffle transition, coinciding with what is expected from the vacancies assisted dislocation climb. In accordance, the threshold stress decreases as the vacancy concentration increases. However, as seen from figure 1(c), the pyramidal type III glide core would require a larger up-climb distance

than the type II core, which consequently renders the core transition more difficult and requiring more vacancy presence in order to achieve the same degree of reduction in the threshold stress in comparison to the type II core, as shown in figure 4. On the other hand, unlike the type II and III cores, we found that the pyramidal type IV glide core may either climb upwards and downwards (along \vec{x}_3) to transform into a shuffle core. As previously mentioned (and illustrated in figure 1(c)), the type IV glide core can climb downwards to transform into a shuffle core even in absence of vacancies. Given that vacancies promote upward dislocation climb, the introduction of vacancies into the pyramidal IV glide core would actually

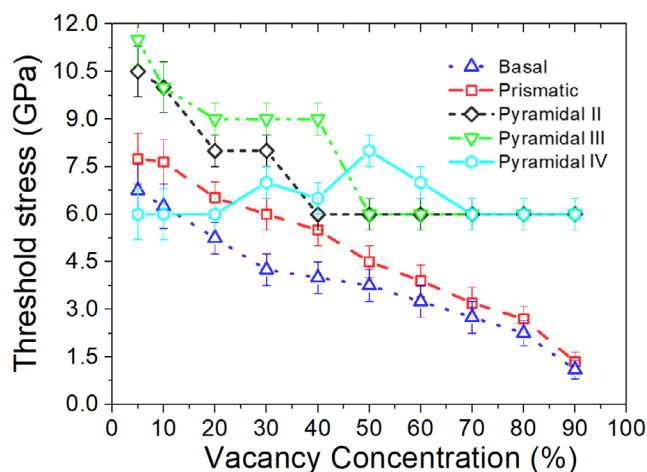


Figure 4. The threshold stress required to initiate dislocation motions of glide cores as a function of vacancy concentrations along the dislocation line obtained from MD simulations.

induce ‘frustration’ in direction of dislocation climb, rendering dislocation segments at different shuffle planes after the glide-to-shuffle core transition (see the supplementary materials for details) and resulting in extra impedance for dislocation motions. At low and high vacancy concentrations, the downwards and upwards dislocation climb motions dominate respectively, while both occur at intermediate vacancy concentrations (see the supplementary materials for details). Consequently for the pyramidal type IV glide core, we see the threshold stress is higher for the intermediate vacancy concentration range.

Further to the GaN system, additional sets of MD simulations have been performed to examine motions of a-type edge dislocations in other wurtzite systems. Our preliminary results (for the representative AlN and InN systems, see the supplementary materials for details) indicate the core structure dependent dislocation mobility and vacancy-assisted core transformation are rather general for wurtzite structured materials.

4. Conclusion

In summary, the present study investigated the core structure dependent dislocation dynamic behaviors of the a-type edge dislocations in wurtzite GaN, employing comprehensive MD simulations. The possible core structures in the three slip systems, i.e. basal, prismatic and pyramidal, have been identified. For dislocations in each slip system, they can be classified into the shuffle and glide sets, corresponding to cores located at two parallel yet inequivalent families of slip planes. It has been found that the dislocation motion is strongly core structure dependent, with the shuffle cores being mobile, while the glide cores being largely immobile due to their extended core structures. Nonetheless, motions of the immobile glide cores can be enabled via a climb-glide process, which can be facilitated by a vacancy-assisted core transition mechanism. The above phenomena were further confirmed to be generally valid for other wurtzite materials, e.g. AlN and InN. Our

findings offer valuable insights for understanding and potential engineering of dislocation behaviors in wurtzite structured materials.

Acknowledgment

We greatly thank the financial support from McGill Engineering Doctoral Award, China Scholarship Council, National Sciences and Engineering Research Council (NSERC) Discovery grant (Grant No. RGPIN-2017-05187), and NSERC Strategic grant (Grant No. STPGP 494012-16). We also acknowledge Supercomputer Consortium Laval UQAM McGill and Eastern Quebec for providing computing power.

ORCID iDs

Cheng Chen  <https://orcid.org/0000-0003-3062-9048>
Pengfei Ou  <https://orcid.org/0000-0002-3630-0385>

References

- [1] Kuykendall T, Ulrich P, Aloni S and Yang P 2007 Complete composition tunability of InGaN nanowires using a combinatorial approach *Nat. Mater.* **6** 951–6
- [2] Perozek J, Lee H P, Krishnan B, Paranjpe A, Reuter K B, Sadana D K and Bayram C 2017 Investigation of structural, optical, and electrical characteristics of an AlGaIn/GaN high electron mobility transistor structure across a 200 mm Si(111) substrate *J. Phys. D: Appl. Phys.* **50** 055103
- [3] Schubert E F and Kim J K 2005 Solid-state light sources getting smart *Science* **308** 1274–8
- [4] Cho C Y, Kwon M K, Park I K, Hong S H, Kim J J, Park S E, Kim S T and Park S J 2011 High-efficiency light-emitting diode with air voids embedded in lateral epitaxially overgrown GaN using a metal mask *Opt. Express* **19** A943–8
- [5] Eddy C R, Nepal N, Hite J K and Mastro M A 2013 Perspectives on future directions in III-N semiconductor research *J. Vac. Sci. Technol. A* **31** 058501
- [6] Chen C, Song P F, Meng F C, Ou P F, Liu X Y and Song J 2018 Predictive modeling of misfit dislocation induced strain relaxation effect on self-rolling of strain-engineered nanomembranes *Appl. Phys. Lett.* **113** 112104
- [7] Mei Y F et al 2009 Fabrication, self-assembly, and properties of ultrathin AlN/GaN porous crystalline nanomembranes: tubes, spirals, and curved sheets *ACS Nano* **3** 1663–8
- [8] Chen C, Song P F, Meng F C, Li X, Liu X Y and Song J 2017 Quantitative analysis and predictive engineering of self-rolling of nanomembranes under anisotropic mismatch strain *Nanotechnology* **28** 485302
- [9] Zeng G S, Tan C K, Tansu N and Krick B A 2016 Ultralow wear of gallium nitride *Appl. Phys. Lett.* **109** 051602
- [10] Sabelfeld K K, Kaganer V M, Pfuller C and Brandt O 2017 Dislocation contrast in cathodoluminescence and electron-beam induced current maps on GaN(0001) *J. Phys. D: Appl. Phys.* **50** 405101
- [11] Tian F F, Liu L, Gu H, Wang J F, Zhang Z Q, Zhou T F and Xu K 2018 Investigation of the reverse recovery characteristics of vertical bulk GaN-based Schottky rectifiers *J. Phys. D: Appl. Phys.* **51** 315101
- [12] Amano H et al 2018 The 2018 GaN power electronics roadmap *J. Phys. D: Appl. Phys.* **51** 163001

- [13] Huang H L, Sun Z H, Cao Y Q, Li F Y, Zhang F, Wen Z X, Zhang Z F, Liang Y C and Hu L Z 2018 Investigation of surface traps-induced current collapse phenomenon in AlGaIn/GaN high electron mobility transistors with schottky gate structures *J. Phys. D: Appl. Phys.* **51** 345102
- [14] Pandey A, Bhattacharya A, Cheng S B, Botton G A, Mi Z T and Bhattacharya P 2018 A dominant electron trap in molecular beam epitaxial InAlN lattice-matched to GaN *J. Phys. D: Appl. Phys.* **51** 14LT01
- [15] Tanikawa T, Ohnishi K, Kanoh M, Mukai T and Matsuoka T 2018 Three-dimensional imaging of threading dislocations in GaN crystals using two-photon excitation photoluminescence *Appl. Phys. Express* **11** 031004
- [16] Mathis S K, Romanov A E, Chen L F, Beltz G E, Pompe W and Speck J S 2001 Modeling of threading dislocation reduction in growing GaN layers *J. Cryst. Growth* **231** 371–90
- [17] Kaganer V M, Jenichen B, Ramsteiner M, Jahn U, Hauswald C, Grosse F, Fernandez-Garrido S and Brandt O 2015 Quantitative evaluation of the broadening of x-ray diffraction, Raman, and photoluminescence lines by dislocation-induced strain in heteroepitaxial GaN films *J. Phys. D: Appl. Phys.* **48** 385105
- [18] Albrecht M, Weyher J L, Lucznik B, Grzegory I and Porowski S 2008 Nonradiative recombination at threading dislocations in n-type GaN: studied by cathodoluminescence and defect selective etching *Appl. Phys. Lett.* **92** 231909
- [19] Matsubara T, Sugimoto K, Goubara S, Inomoto R, Okada N and Tadatomo K 2017 Direct observation of inclined a-type threading dislocation with a-type screw dislocation in GaN *J. Appl. Phys.* **121** 185101
- [20] Saito W, Noda T, Kuraguchi M, Takada Y, Tsuda K, Saito Y, Yamaguchi M and Omura I 2009 Effect of buffer layer structure on drain leakage current and current collapse phenomena in high-voltage GaN-HEMTs *IEEE Trans. Electron Devices* **56** 1371–6
- [21] Hsu J W P, Manfra M J, Lang D V, Richter S, Chu S N G, Sergeant A M, Kleiman R N, Pfeiffer L N and Molnar R J 2001 Inhomogeneous spatial distribution of reverse bias leakage in GaN Schottky diodes *Appl. Phys. Lett.* **78** 1685–7
- [22] Reynolds C L, Reynolds J G, Crespo A, Gillespie J K, Chabak K D and Davis R F 2013 Dislocations as quantum wires: Buffer leakage in AlGaIn/GaN heterostructures *J. Mater. Res.* **28** 1687–91
- [23] Moram M A, Sadler T C, Haberen M, Kappers M J and Humphreys C J 2010 Dislocation movement in GaN films *Appl. Phys. Lett.* **97** 261907
- [24] Zeng G S, Sun W, Song R B, Tansu N and Krick B A 2017 Crystal orientation dependence of gallium nitride wear *Sci. Rep.* **7** 14126
- [25] Zeng G S, Tansu N and Krick B A 2018 Moisture dependent wear mechanisms of gallium nitride *Tribol. Int.* **118** 120–7
- [26] Xin Y, Pennycook S J, Browning N D, Nellist P D, Sivanathan S, Omnes F, Beaumont B, Faurie J P and Gibart P 1998 Direct observation of the core structures of threading dislocations in GaN *Appl. Phys. Lett.* **72** 2680–2
- [27] Potin V, Ruterana P, Nouet G, Pond R C and Morkoc H 2000 Mosaic growth of GaN on (0001) sapphire: a high-resolution electron microscopy and crystallographic study of threading dislocations from low-angle to high-angle grain boundaries *Phys. Rev. B* **61** 5587–99
- [28] Liliental-Weber Z, Zakharov D, Jasinski J, O'Keefe M A and Morkoc H 2004 Screw dislocations in GaN grown by different methods *Microsc. Microanal.* **10** 47–54
- [29] Weingarten N S and Chung P W 2013 a-Type edge dislocation mobility in wurtzite GaN using molecular dynamics *Scr. Mater.* **69** 311–4
- [30] Matsubara M, Godet J, Pizzagalli L and Bellotti E 2013 Properties of threading screw dislocation core in wurtzite GaN studied by Heyd–Scuseria–Ernzerhof hybrid functional *Appl. Phys. Lett.* **103** 262107
- [31] Belabbas I, Chen J, Belkhir M A, Ruterana P and Nouet G 2006 New core configurations of the c-edge dislocation in wurtzite GaN *Phys. Status Solidi c* **3** 1733–7
- [32] Bere A and Serra A 2002 Atomic structure of dislocation cores in GaN *Phys. Rev. B* **65** 205323
- [33] Bere A, Chen J, Ruterana P, Serra A and Nouet G 2002 The atomic configurations of the a→ threading dislocation in GaN *Comput. Mater. Sci.* **24** 144–7
- [34] Northrup J E 2001 Screw dislocations in GaN: the Ga-filled core model *Appl. Phys. Lett.* **78** 2288–90
- [35] Chen C, Meng F C and Song J 2016 Effects of Mg and Al doping on dislocation slips in GaN *J. Appl. Phys.* **119** 064203
- [36] Chen C, Meng F C and Song J 2015 Core structures analyses of (a plus c)-edge dislocations in wurtzite GaN through atomistic simulations and Peierls–Nabarro model *J. Appl. Phys.* **117** 194301
- [37] Justo J F, de Koning M, Cai W and Bulatov V V 2000 Vacancy interaction with dislocations in silicon: the shuffle-glide competition *Phys. Rev. Lett.* **84** 2172–5
- [38] Weingarten N S 2018 Dislocation mobility and Peierls stress of c-type screw dislocations in GaN from molecular dynamics *Comput. Mater. Sci.* **153** 409–16
- [39] Belabbas I, Chen J, Heggie M I, Latham C D, Rayson M J, Briddon P R and Nouet G 2016 Core properties and mobility of the basal screw dislocation in wurtzite GaN: a density functional theory study *Model. Simul. Mater. Sci. Eng.* **24** 075001
- [40] Kamimura Y, Edagawa K and Takeuchi S 2013 Experimental evaluation of the Peierls stresses in a variety of crystals and their relation to the crystal structure *Acta Mater.* **61** 294–309
- [41] Moram M A, Oliver R A, Kappers M and Humphreys C J 2009 The spatial distribution of threading dislocations in gallium nitride films *Adv. Mater.* **21** 3941
- [42] Cheng C, Fanchao M, Pengfei O, Guoqiang L, Bing L, Huicong C, Qiwen Q and Jun S 2019 Effect of indium doping on motions of (a)-prismatic edge dislocations in wurtzite gallium nitride *J. Phys.: Condens. Matter* **31** 315701
- [43] Plimpton S 1995 Fast parallel algorithms for short-range molecular-dynamics *J. Comput. Phys.* **117** 1–19
- [44] Stillinger F H and Weber T A 1985 Computer-simulation of local order in condensed phases of silicon *Phys. Rev. B* **31** 5262–71
- [45] Zhou X W, Foster M E, van Swol F B, Martin J E and Wong B M 2014 Analytical bond-order potential for the Cd–Te–Se ternary system *J. Phys. Chem. C* **118** 20661–79
- [46] Gruber J, Zhou X W, Jones R E, Lee S R and Tucker G J 2017 Molecular dynamics studies of defect formation during heteroepitaxial growth of InGaIn alloys on (0001) GaN surfaces *J. Appl. Phys.* **121** 195301
- [47] Zhou X W, Chavez J J, Almeida S and Zubia D 2016 Understanding misfit strain releasing mechanisms via molecular dynamics simulations of CdTe growth on {112} zinc-blende CdS *J. Appl. Phys.* **120** 045304
- [48] Zhou X W, Ward D K, Zimmerman J A, Cruz-Campa J L, Zubia D, Martin J E and van Swol F 2016 An atomistically

- validated continuum model for strain relaxation and misfit dislocation formation *J. Mech. Phys. Solids* **91** 265–77
- [49] Zhou X W, Ward D K, Martin J E, van Swol F B, Cruz-Campa J L and Zubia D 2013 Stillinger-weber potential for the II–VI elements Zn–Cd–Hg–S–Se–Te *Phys. Rev. B* **88** 085309
- [50] Zhou X W, Jones R E and Gruber J 2017 Molecular dynamics simulations of substitutional diffusion *Comput. Mater. Sci.* **128** 331–6
- [51] Chu K, Gruber J, Zhou X W, Jones R E, Lee S R and Tucker G J 2018 Molecular dynamics studies of InGaN growth on nonpolar (11 $\bar{2}$ 0) GaN surfaces *Phys. Rev. Mater.* **2** 013402
- [52] Hull D and Bacon D J 2001 *Introduction to Dislocations* (New York: Elsevier)
- [53] Bulatov V and Cai W 2006 *Computer Simulations of Dislocations* (Oxford: Oxford University Press)
- [54] Nocedal J and Wright S J 2006 *Conjugate Gradient Methods* (Berlin: Springer)
- [55] Xiang H G, Li H T, Fu T, Huang C and Peng X H 2017 Formation of prismatic loops in AN and GaN under nanoindentation *Acta Mater.* **138** 131–9